

Article |

The influence of additions on the electrodeposition of the alloy of Co - Zn from a new eutectic deep solvent

Shymaa Hussien Al-Said^{1*}, **Azhar Y.M. Al-Murshedi**²

¹*Thi-Qar General Directorate of Education, Ministry of Education, Thi-Qar, Iraq.*

Shymaah.alsaadi@student.uokufa.edu.iq

²*Department of Chemistry, Faculty of Education for Girls, University of Kufa, Kufa, Iraq.*

Azhar.almurshidi@uokufa.edu.iq

***Corresponding Author:** *Shymaa Hussien Al-Said, 1Thi-Qar General Directorate of Education, Ministry of Education, Thi-Qar, Iraq, E-mail:*

Shymaah.alsaadi@student.uokufa.edu.iq

Abstract

E-coating deposition of Co-Zn alloys presents a promising approach for creating multifunctional coatings that simultaneously enhance mechanical properties and corrosion resistance. In this study, a novel eutectic deep solvent (DES) composed of lithium chloride and 1,3-propanediol was developed and maintained at 80°C. This solvent was utilized for electrodepositing Co-Zn alloy coatings onto copper substrates. The coatings' composition, phase structure, and morphology were characterized using field emission scanning electron microscopy (FE-SEM), atomic force microscopy (AFM), and X-ray diffraction (XRD). Electrochemical properties were assessed through cyclic voltammetry (CV) to investigate the effects of deposition temperature on composition and structural changes. Co-deposition of zinc and cobalt was achieved under galvanostatic conditions, resulting in high-quality Co-Zn alloy coatings with a compact morphology and a single phase when deposited at 80°C, with a current density of 0.012 mA/cm² over a duration of 2 hours. Additionally, the efficiency of the electrodeposition process improved with the incorporation of additives, specifically 10% H₂O, TX100, and TW20.

Keywords: Electrodeposition, Co - Zn alloy coatings, an eutectic deep solvent (DES), 1, 3-Propanediol, surface morphology, electrochemical properties, Lithium Chloride, additives

Introduction

The literature concerning the electrodeposition of zinc-nickel alloy coatings has received a great deal of attention [1],[2],[3]. This merits their superb properties such as corrosion resistance, paintability and high formability [4],[5],[6]. These alloys have been used extensively in many applications such as vehicles, aviation, shipping, building and electronics, but because of the complexity of co-deposition mechanisms, the deposition processes are still not understood [7]. Electrodeposition technology enables control of the surface coverage and thickness, chemical composition, and microstructure of materials by means of varying the deposition conditions like current density, pH, and composition bath [8]. The reasons why electrodeposition is simply the most preferred electrochemical method for preparing coatings is because of the simplicity or its moderate cost, and great efficiency. Its simplicity in controlling the thickness and chemical composition of the coatings is carried out by the changes in deposition conditions, current density, pH value and the composition bath. And because the reduction of metallic cations [9] results in driving the deposition of the coating onto a substrate that is cathodic. The most popular metal coating is zinc (Zn), which is used in electroplating, or galvanizing. Zincate represents a green candidate, banded Fe-Zn alloys with electroplating as the method of manufacturing that are better Zn corrosion resistant [10],[11],[12],[13],[14]. Also, less hydrogen embrittlement and uniform deposition of plating layers are beneficial in zincate solution. Also, the bath solution is less aggressive to the equipment [15]. These alloys appear to be better than cadmium (Cd), which is toxic to a considerable extent, because they are Zinc plus zincate negative alloying, cyanide based electrolytic deposition, copper/iron alloyed electrodes negative zinc electrodes interface [6],[16]. due positioned through electrodeposition process are in combination more positive than pure zinc and have other negative impacts with the use of cyanide containing electrolytes in the electrodeposition processes which are detrimental and may cause varying damage to health and the environment [6],[17],[18],[19]. To address the problem of corrosion of ferrous substrates, which they are of course more; therefore, zinc sacrificial coatings were designed. In various engineering fields, Zinc sacrificial coatings have been widely used in place of Cadmium in highly corrosive conditions or with long service life. But in order to provide cadmium-like corrosion protection, a thicker coating is needed because of zinc's rather high corrosion rate. This stimulated research directed towards the development of alloy coatings with small proportions of other constituents such as manganese and iron, cobalt, tin, nickel, [20],[21],[22],[23] with the aim of altering the corrosion rate and corrosion potential. In the case of steels protected by galvanic zinc, there will remain anodic behavior, and therefore sacrificial protection will be preserved, while the less severe corrosion rate will counteract corrosion for a longer period of time. In this study,

in order to to minimize environmental impact during the electrodeposition process and solvent use by developing a new environmentally friendly deep eutectic solvent (a fourth type) that is rarely employed in coating applications. This solvent was created by replacing choline chloride with lithium chloride and mixing it with 1,3-propanediol in an equivalent ratio of 1:4. The electroplating process focused on the deposition of cobalt and Co-Zn alloys. Additionally, we incorporated specific additives, as their presence is crucial for influencing deposit growth and structure, which ultimately enhance the appearance and properties of the coatings, as well as the performance of the electroplating bath.

Experimental

Chemical and Materials

The following chemicals were purchased from Sigma Aldrich and used without further purification: 1,3- propanediol ($C_3H_8O_2$, > 99.8%) and lithium chloride ($LiCl$, $\geq 98\%$). using The cobalt salts; $CoCl_2 \cdot 6H_2O$ (Aldrich $\geq 98\%$), and the zinc salts; $ZnCl_2$ (Aldrich $\geq 99\%$). Triton x100 (Tx100, 0.02 M) (Aldrich - Sigma, 99%) and Tween 20 (Tw20, 0.01 M) (Aldrich – Sigma $\geq 99.5\%$) were the additives used.

Preparation of electrolyte

Two components were combined and stirred at 80 °C to create a homogenous, colorless liquid, which is the eutectic mixture $LiCl$: 1,3propanediol (1:4 molar ratio), This is done by dissolving 10 g of lithium chloride with 144.76 g of 1,3 propanediol on a hot plate at 80 °C for two hours while stirring constantly until a homogenous, colorless liquid solution is produced, density and conductivity of new DES at 25°C (1.093) , (1.2) respectively.

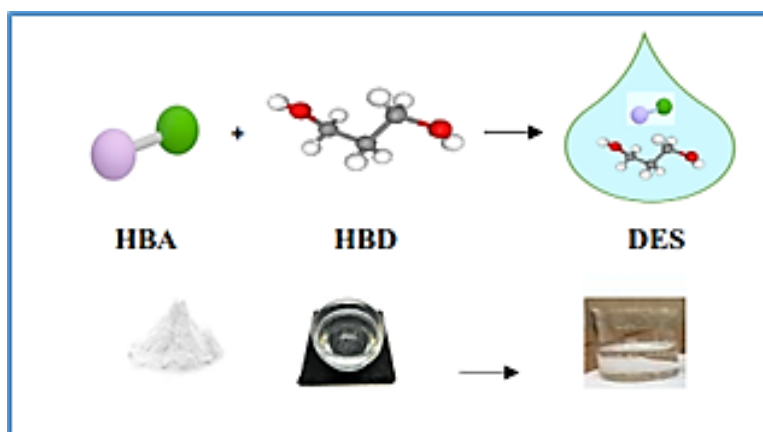


Figure1. Shows the new DES preparation

Electrochemical analysis and electrodeposition

Using auto lab/PGSTAT12 potentiostat linked with GPES2 software, the cyclic voltammetry studies were done. A three electrode system, comprising of a working electrode (platinum, 1.3 cm diameter), flag counter electrode (platinum) and silver wire reference electrode. Each working electrode was polished with a γ -alumina paste of 0.05 μm , and distilled water was run before every experiment. Each cyclic voltammogram was recorded at 80 °C and within a scan rate of 10 mV/s to 60 mV/s. Copper substrates in deep eutectics was electroplated with 0.3 M ZnCl_2 and 0.4 M CoCl_2 in both presence and absence of additives. LiCl: (1,3-propanediol) based liquid will create $[\text{MCl}_4]^{-1}$ by dissolving MCl_2 (M= Zn, Co) in 1:4 molar ratio. The cathodic plates (Cu substrate) were physically polished, rinsed in water, and dried before being used in bulk electrolysis. Anode was iridium oxide coated titanium mesh electrode, 40mm x 50mm, prepared in identical manner. In all studies, solution temperature was at 80 ° C, and substrate was deposited with a continuous current for two hours. The substrates were subsequently removed from the solution and water rinsed, as presented in figure 2 below:

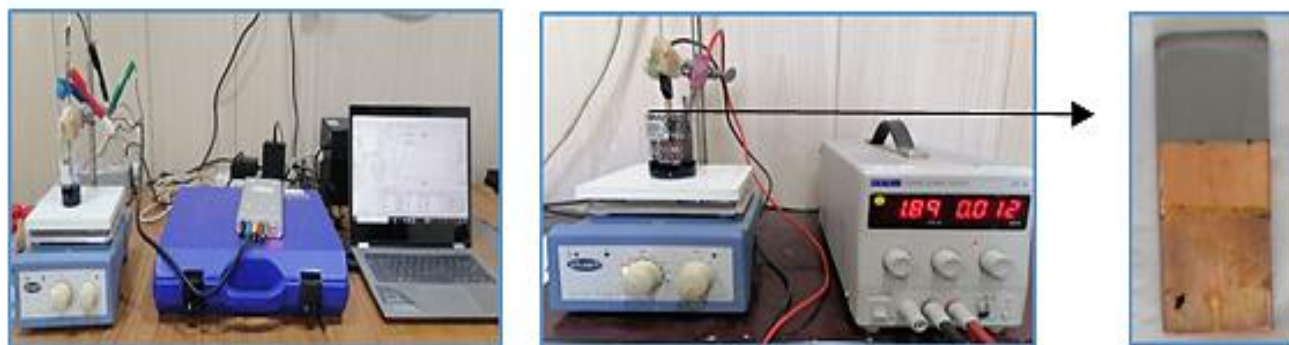


Figure 2. Shows electrochemical electrodeposition of Co-Zn alloy

Surface analysis

The Field emission-scanning electron microscopy (FE - SEM) investigated surface characterisation; metal analysis of the plating compositions was conducted by (EDX); powder X-ray diffraction technique was applied to investigate XRD pattern of the Co-Zn deposits

Results and Discussion

Cyclic voltammetric (CV) studies

We researched the redox of Zn, Co and Co-Zn in a novel DES with cyclic voltammetry method. The third figures shows in an entirely new DES the individual cycle voltammetric for 0.3 M ZnCl_2 and 0.4 M $\text{CoCl}_2 \cdot 6\text{H}_2\text{O}$. In the figure, the experiments were conducted at an 80 degrees centigrade and 30mVs^{-1} , making use of three electrodes. The voltageammogram between Co and Zn demonstrate that Co

reduction started at approximately 0.7 V, however, the oxidation peak for Co was near 0.2 V and his toric Zn reduction began at 1.1 V with primary oxidation current peak of 0.3 V. The results of Pereira et al. [24],[25] assist in corroborating this thinking, With every relative comparison of the voltammogram enclosing Zn and Co, it is certain that a greater amount of energy is needed to reduce the Zn species than Co species. The difference in Zn and Co deposition behavior is noted in the relevant figure. It is important to mention that above a particular voltage, cobalt ions in the electrolyte are reduced first on the electrode surface, and then zinc ions. Cobalt starts depositing at about 0.7V and continues until zinc begins depositing at 1.1V.

In the case of cobalt metal dissolving, it requires a more negative value of potential than zinc oxidation which takes place at 1.1 V while cobalt dissolution occurs at 0.2 V. It shows cobalt is more resistant to corrosion than zinc, thus it can be used for cathodic protection of zinc. Cyclic voltammograms (C.V) of the deep eutectic solvent (DES) that has 0.3 M ZnCl_2 and 0.4 M $\text{CoCl}_2 \cdot 6\text{H}_2\text{O}$ shows two clear deposition peaks which are distinct from each other. Cobalt deposition is marked with the initial peak of 0.7 V and zinc deposition is marked with the second reduction peak of 1.3 V. Peaks for dissolution of zinc and cobalt for the electrode were noted around 0.7 V and 1.4 V, which correspond to the anodic peaks. The C.V data verifies the existence of independent reduction peaks for Zn and Co, which is also in agreement with literature data. As a result, it is improbable for a Co-Zn alloy to form immediately upon deposition. The process seems to take place through the mutual Co-deposition of zinc and cobalt, which is illustrated in the figure.

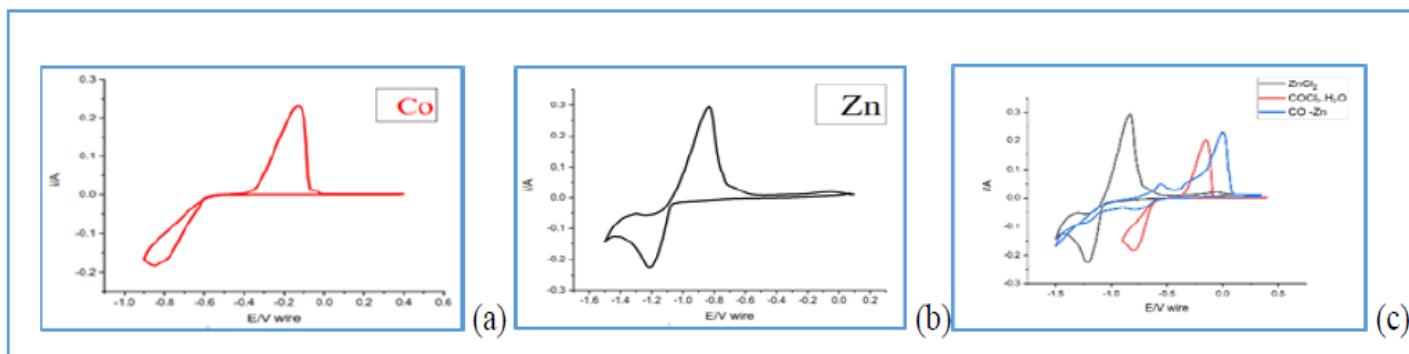


Figure 3: Cyclic voltammograms of Co-Zn, Zn, and Co obtained (a) in DES from 0.3 M ZnCl_2 , (b) from 0.4 M $\text{CoCl}_2 \cdot 6\text{H}_2\text{O}$, and (c) from 0.3 M ZnCl_2 and 0.4 M $\text{CoCl}_2 \cdot 6\text{H}_2\text{O}$ in DES.

A. Voltammetry of Intermetallic Co-Zn, Zn, and Co alloy with/without additives

The incorporation of certain additives in a fresh deep eutectic solvent (DES) containing Zn, Co, and Co-Zn was analyzed through the study of cyclic voltammograms

as shown in Figure 4. The addition of H₂O and TX100 led to a noticeable intensification of the redox peak of Zn, as shown in Figure 4(a). Likewise, Co also exhibited a similar trend with the redox peaks becoming more pronounced with the introduction of H₂O and TX100 as illustrated in Figure 4(b). This behavior can be attributed to an increase in the solution's conductivity. The investigation further elaborated on the Co-Zn system and revealed that these additives shifted the redox potential. The stripping peaks of Co-Zn had greater intensity due to the presence of H₂O and TX100, which also caused the reduction potential to shift to more negative values. This indicates that water seems to play a major role in affecting the Co-Zn redox system's electrolytic behavior. Moreover, Figure 4 shows that with the addition of H₂O and TX100 to the solution during the electrodeposition of the Zn-Co alloy, a wider redox peak was observed. This phenomenon may be related to the post-alloyed electrodeposition resistance, thus illustrating the nature of the additives on the deposition process.

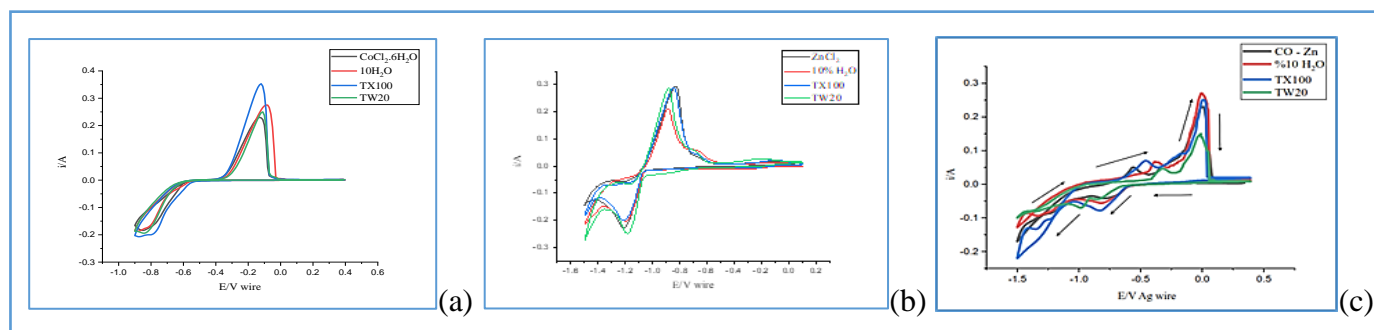


Figure 4. Cyclic voltammograms of Co-Zn, Zn, and Co produced by: (a) 0.3M ZnCl₂ in EDS for (b) 0.4M CoCl₂. 6H₂O and (c) 0.3M ZnCl₂ and 0.4 M CoCl₂. 6H₂O in EDS with and without additives.

B. Temperature impact on voltammetry of Co-Zn alloy, Zn (II) and Co (II)

Cobalt-Zinc alloy electrodeposition was achieved at high temperatures of 80 °C. The electrodeposition of 0.3 M ZnCl₂, 0.4 M CoCl₂.6H₂O, and Co – Zn in a fresh deep eutectic solvent (LiCl+1,3-propanediol) is shown in Figures 5 from 30 to 80 °C. The cyclic voltammetry C.V of Co and Zn with ZnCl₂ & CoCl₂.6H₂O were conducted in novel DES at different temperatures, and all the tests were conducted at a scan rate of 30 mv/s. The cyclic voltammograms of Co-Zn in which significant increase in strength of its reduction and dissolutions peaks is observed at high temperatures 80 °C is shown in figure 5(c). Furthermore, It is observed in figure 5(a, b) that significant positive change of the reduction potentials of zinc and cobalt is obtained when temperature is increased. First of all, it was hypothesized that increasing the temperature of the solution would decrease the viscosity leading to better mass transfer towards the electrode surface. It

would also increase the free void volume of the solution. The viscosity and conductivity of the bath liquid are important components of electrochemical processes, and temperature influences both of them. DES viscosity is determined by free volume; therefore, higher temperature results in greater mobility of the ionic species within the liquid. Therefore, oxidation/reduction reactions can be expedited by high temperature, as shown in this figure (5), through increasing mass transport toward the electrode surfaces.

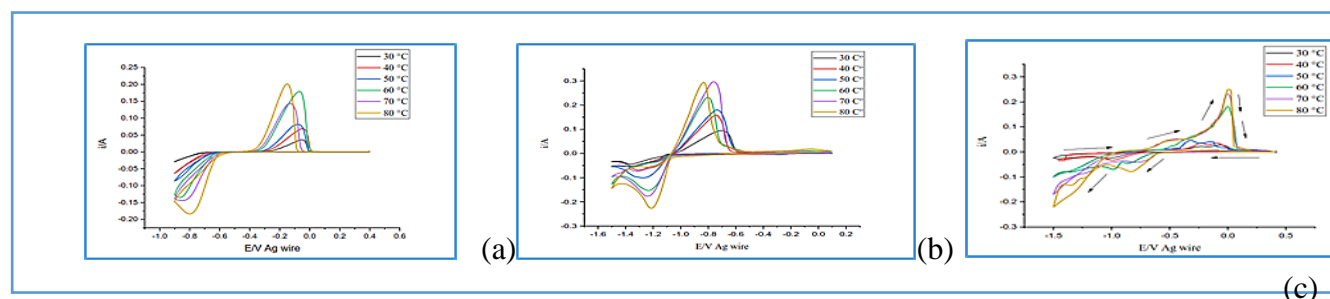


Figure 5. Voltammograms obtained from a new DES with 0.3M ZnCl_2 , 0.4M $\text{CoCl}_2 \cdot 6\text{H}_2\text{O}$, and Co-Zn alloy at different temperatures on a platinum electrode (1.0mm diameter) with a scan rate of 30 mV s^{-1} with respect to Ag/ AgCl reference electrode.

Co-Zn coating and electroplating processes

We analyzed the morphology of each metal deposit using SEM imaging. The SEM images in Figure 6 compare the morphologies of zinc, cobalt, and cobalt-zinc alloy films grown from fresh deep eutectic solvent (DES). As can be seen in Fig. 6a and 6b, a pure zinc film takes the Shape of coral reefs and a pure cobalt coating has spherical agglomerates. Co-Zn crystallites adopted the shape of pine trees (6c). DES at $80 \text{ }^\circ\text{C}$ for 2 hours with a current of 0.012 mA cm^{-2} was able to complete all of the copper surface depositions on the electrodes. It is quite evident that the average particle size of the Zn deposits and Co deposits is different. Appeared in SEM, deposit 6c, the Co-Zn coating looks quite different than the cobalt and zinc coatings alone, which leads to one possibility. This reason could be due to some other speciation of the electrolyte or different composition of the coating. From this figure 6 and the XRD analysis (Fig. 9), it can be noticed that the phase structure of the Co-Zn film is observable, thus this instrument is the most likely one to determine whether this is an alloy or not.

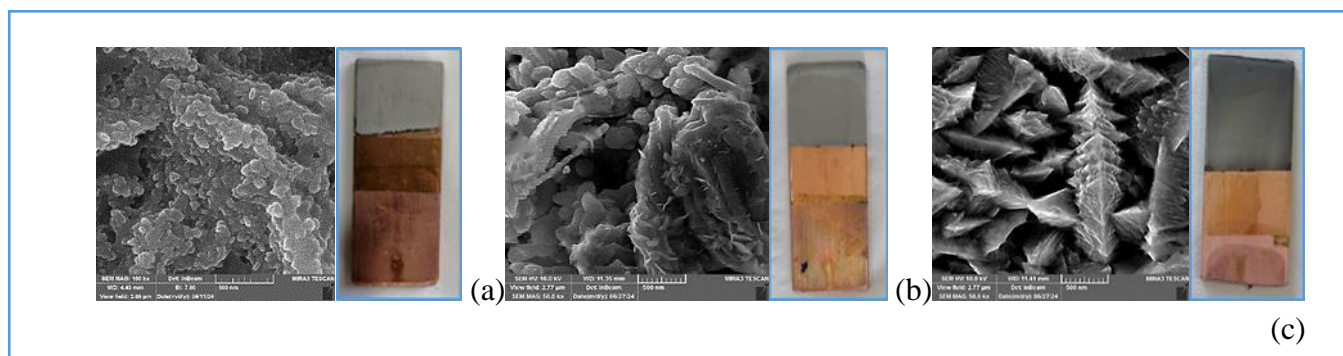


Figure 6. SEM imaging of the electrodes shows the deposits for (a) 0.4M $\text{CoCl}_2 \cdot 6\text{H}_2\text{O}$, (b) 0.3M ZnCl_2 and (c) Co-Zn obtained from a new EDS with 0.4M $\text{CoCl}_2 \cdot 6\text{H}_2\text{O}$ and 0.3M ZnCl_2 , no other additions. All depositions have been achieved from a newly prepared EDS on copper substrate at 80°C after 2 hours of 0.012 mA cm^{-2} current.

Effect of Additives on Morphology of Co-Zn Deposit

A. FE - SEM

The Optical photograph and SEM image of the Co-Zn alloy deposits is shown in the Figures. Co-Zn alloy deposits were formed in fresh deep eutectic solvent (DES) containing 0.3 M ZnCl_2 and 0.4 M $\text{CoCl}_2 \cdot 6\text{H}_2\text{O}$ with some additions of 0.02 M TritonX100, 0.01 M Tween20 and 10% H_2O . The deposits were made on VII. Cu substrates by direct current electrolysis at 0.012 mA cm^{-2} for 2 hours. Graph Figure 7(a) shows that there was obtained dark gray rough Co-Zn alloy deposit from the electrolyte containing no additions. Here it is obvious that the Co-Zn particles which precipitated had different sizes but appeared to be of random shape. As demonstrated in Figs. 7(a), 7(b), 7(c), and 7(d) there are distinct changes in roughness and morphology of the Co-Zn deposit observed when the additives were put in the container with Co-Zn bath separately. The Figures 7(a) and 6(a) show semifinished rough dark gray Co and Co-Zn alloy deposit issued from electrolyte containing no additions with random size distribution of Co and Co-Zn particles. In Figures 7(a) and 6(b), the roughness and morphologies of Co and Co-Zn deposits were notably different after the use of the additives to the Zn and Co-Zn baths. Typically, TX100 is employed in the electrodeposition of metals in order to improve the coating properties. In this study, a specific change in the morphology of the Co-Zn film was observed in the use of TX100 during the electrodeposition of Co-Zn. The deposition process yielded a stunning Co-Zn film when done in a bath with TX100, and a notable increase in smoothness and some refinement in the coating's grain structure was observed in Figure 7(c). One might suggest that TritonX-100 slows the Zn deposition rate by forming an adsorbed layer on the cathodic electrode surface.

Using TritonX-100 as an addition has helped to increase the smoothness and refinement in the grain size of the Zn deposit as seen in Fig. 7(c). TritonX-100 can thus be a quite useful brightener in Zn deposition. Photographs and morphologies of the Co-Zn deposits acquired from a system with 10% of H₂O are shown in Fig. 7(b). It is abundantly evident that adding water produces a smoother surface finish that is, more uniform and finer grained deposits. Photographs and morphologies of the Co-Zn deposits acquired from a system with 0.01M of TW20 are shown in Fig. 7(d), where it is evident the big-sized Co-Zn particles were formed with a lot more random shape as seen in this figure (7).

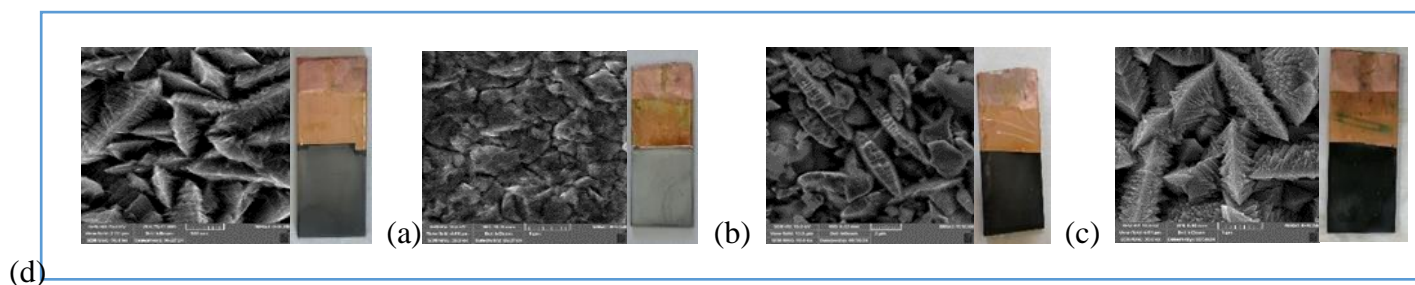


Figure 7. FE-SEM showing Co-Zn electroplating in a new Deep Eutectic Solvent (DES) containing 0.4 M ZnCl₂ and 0.3 M CoCl₂.6H₂O using (a) no additives, (b) 10% H₂O, (c) TX100, and (d) TW20.

B. AFM

AFM imaging the nucleation, topography, and roughness of Co-Zn deposits are shown in figures 8 that include and do not include the use of additives. The micrographs reveal the presence of Co and Zn granules obtained in Co-Zn deposits which rudimentarily appear to the eyes. Particularly for the case for deposition from a system with additives, as shown in Figure 8(b), 7(c), and 8(d), Co-Zn particles of very small dimensions are manifest. The coating made from the electrolyte without the addition of Co-Zn roughness calculated to be approximately 54.95 nm. It was noted that the roughness of the deposit decreased by 34.18 nm when the electrolyte was changed to one containing TX100. The Co-Zn film deposited also had its roughness decreased to 32.88 nm with the addition of water. These additives could act as levelers in this case. Some of them which adsorb on the electrode surface could block the higher portions of the surface.

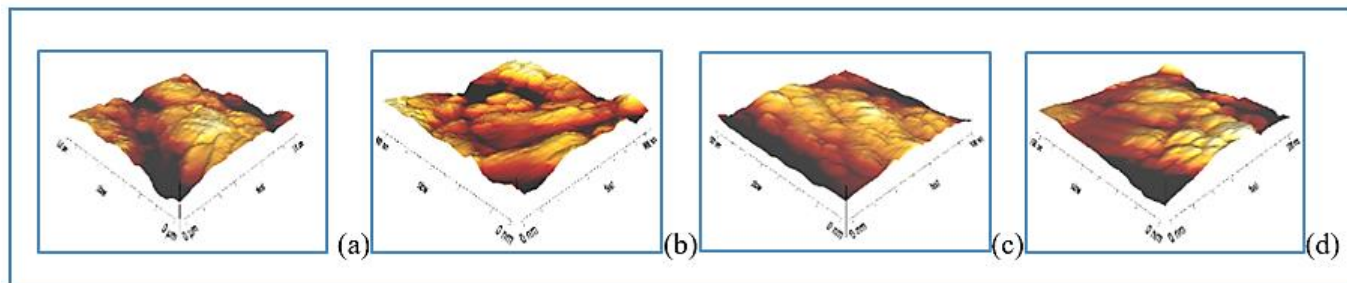


Figure 8. AFM of Co- Zn electroplating in a new DES holding 0.4 M ZnCl₂ and 0.3M CoCl₂. 6H₂O in the attendance of (a) no additives, (b) 10% H₂O, (c) TX100, and (d) TW20.

Table 1. In the with and without of additives, the smoothness of Co-Zn films produced in DES

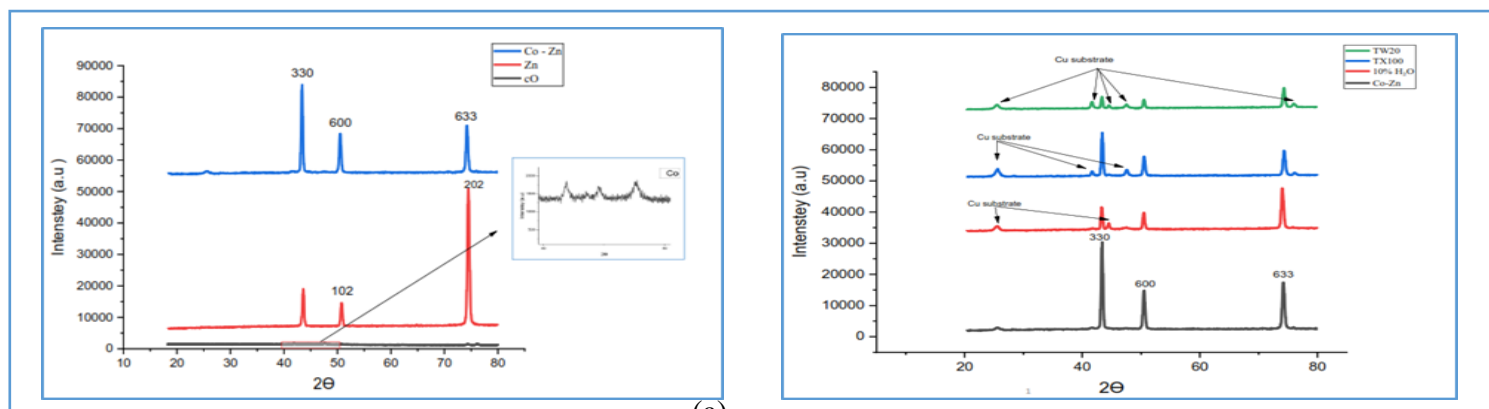
Metal salt	Additives	Roughness, Ra/nm	Average particle size /nm
Zn-Co	Non.	54.95	67.20
Zn-Co	With 10%	32.88	39.57
Zn-Co	With TX100	34.18	40.91
Zn -Co	With TW20	29.20	37.30

Table 2. The EDAX analysis results, when using ratio of Co-Zn films in the with and without of additives

Co-Zn coating	Co% Wt.	Zn% Wt.
Non	19.83	80.13
With 10% H ₂ O	69.42	30.58
With TX100	52	48
With TW20	24.7	75.3

C. X-ray diffraction (XRD)

The purpose of this study is to analyze the XRD results concerning the CoZn deposits crystallized from systems both with and without the additive. XRD was performed to check whether an alloy formed in all cases. The results are shown in Figures 9 which illustrates the XRD spectra of Co-Zn deposits without additives and Co-Zn deposits employing H₂O, TX100 and TW20. An XRD pattern of Co-Zn deposits from the system without additions showed a range of Zn and Co planes such (101), (102), and (202). Co was found to be at 2kappa values of 43.04, 45.8, 47.8 with planes of (100%), (111%), and (101%), were revealed at 2 theta values of 13.45, 15.37, 27.34, 44.64, 51.82, 73.81. While the other Co-Zn coatings where Zn diffraction peak (101), Zn diffraction peak was observed in master Co-Zn deposited system when the deposition was done from a system with additives at 2 theta values of 44.64 and 51.82. This was discovered of the Co-Zn deposited system. The diffraction peak Zn (101)(102) of the Co-Zn coating formed from the system without additives was observed at 2 theta 44.04 and 51.32. This implies that the new face formed in the electrolyte contending TX100 and H₂O. Shown is the X ray diffraction analysis of a Co-Zn alloy coating deposited over Cu substrates from DES containing these additives at 80 degrees C and current density of 0.012 mA/cm².



(b)

(a)

Figure 9. Using 0.3 M ZnCl₂ and 0.4 M CoCl₂.6H₂O, XRD patterns of Zn electro-deposited, Co electro-deposited, and Co-Zn electro-deposited without additives; XRD patterns of Co-Zn electro-deposited in DES by means of additives.

Conclusion

This effort aimed to create a new deep eutectic solvent (DES) and apply it on copper (Cu) substrate for Co-Zn alloy electrodeposition. The work investigates Co-Zn alloy electrodeposition in relation to additives including H₂O, TritonX100, and Tween20. Many elements have affected the electrochemical coating of Co-Zn alloys. Comparatively to the same solution without the addition, this experiment showed that the additions significantly raised the alloy deposition in this system. Significant changes in the cyclic voltammetry for Co-Zn alloy resulted from the addition to the Co-Zn-containing solution. We found in the Co-Zn cyclic voltammetry experiments that TritonX100 and H₂O both induce an increase in the reduction peak. XRD was used to investigate the crystal structures of the Co-Zn deposits so generated; variations in Co and Zn diffraction peak strength were observed upon deposition from electrolytes including additives. AFM investigations indicate that several additives, like TritonX100 and H₂O, have great impact on improving the coating for Co-Zn alloy when electrodeposition is conducted with additive present in the electrolyte. The surface roughness and grain sizes of the subsequent deposition have shown a notable drop. The FE-SEM results show that on copper (Cu) substrate strong deposition and adhesion, TritonX100 and H₂O produced Co-Zn alloy. The deposition occurring in new DES at 80 °C produced hard adherent Co-Zn coating; the inclusion of additives is advantageous for the final coating.

Acknowledgements

This work was made possible by Supervisor Dr. Azhar Y. M. Al-Morshedi providing the required electrochemical materials and equipment, as well as by the assistance and direction from Supervisor.

References

- [1] Maniam, K. K., & Paul, S. (2020). Progress in electrodeposition of zinc and zinc nickel alloys using ionic liquids. *Applied Sciences*, 10(15), 5321.
- [2] Yavuz, A., Yilmaz Erdogan, P., Zengin, H., & Zengin, G. (2022). Electrodeposition and Characterisation of Zn-Co Alloys from Ionic Liquids on Copper. *Journal of Electronic Materials*, 51(9), 5253-5261.
- [3] Lotfi, N., Aliofkhazraei, M., Rahmani, H., & Darband, G. B. (2018). Zinc–nickel alloy electrodeposition: characterization, properties, multilayers and composites. *Protection of metals and physical chemistry of surfaces*, 54, 1102-1140.
- [4] Maniam, K. K., & Paul, S. (2021). Corrosion performance of electrodeposited zinc and zinc-alloy coatings in marine environment. *Corrosion and Materials Degradation*, 2(2), 163-189.
- [5] Zade, G. S., & Patil, K. D. (2024). Advances in corrosion-resistant coatings: Types, formulating principles, properties, and applications. *Functional Coatings: Innovations and Challenges*, 110-152.
- [6] Falcón, J. M., & Aoki, I. V. (2024). Electrodeposition of ZnCo alloy coatings on carbon steel and their corrosion resistance. *Surface and Coatings Technology*, 481, 130603.
- [7] Raabe, D. (2023). The materials science behind sustainable metals and alloys. *Chemical reviews*, 123(5), 2436-2608.

- [8] Chen, Y., Yang, H., Feng, H., Yang, P., Zhang, J., & Shu, B. (2023). Electrodeposition and corrosion performance of Ni-Co alloys with different cobalt contents. *Materials Today Communications*, 35, 106058.
- [9] Anwar, S., Zhang, Y., & Khan, F. (2018). Electrochemical behaviour and analysis of Zn and Zn–Ni alloy anti-corrosive coatings deposited from citrate baths. *RSC advances*, 8(51), 28861-28873.
- [10] Cao, F., Wang, J., Lian, Y., Wang, Y., Wang, X., Wang, X., ... & Shi, L. (2023). A Study on the Influence of the Electroplating Process on the Corrosion Resistance of Zinc-Based Alloy Coatings. *Coatings*, 13(10), 1774.
- [11] Ma, H. R., Chen, X. Y., Li, J. W., Chang, C. T., Wang, G., Li, H., ... & Li, R. W. (2017). Fe-based amorphous coating with high corrosion and wear resistance. *Surface Engineering*, 33(1), 56-62.
- [12] Yan, F., Zhang, K., Yang, B., Chen, Z., Zhu, Z., & Wang, C. (2021). Interface characteristics and reaction mechanism of steel/Al welds produced by magnetic field assisted laser welding-brazing. *Optics & Laser Technology*, 138, 106843.
- [13] Wang, K., Yin, X., Li, C., & Du, K. (2023). Effect of Zn on Phase Evolution and Shear Resistance of Stainless Steel and Aluminum Alloy Interface by Laser Cladding. *Coatings*, 13(7), 1267.
- [14] Zhou, W., & Xu, C. (2024). Effect of heating process on the corrosion resistance of zinc iron alloy coatings. *High Temperature Materials and Processes*, 43(1), 20240014.
- [15] Sadananda, K., Yang, J. H., Iyyer, N., Phan, N., & Rahman, A. (2021). Sacrificial Zn–Ni coatings by electroplating and hydrogen embrittlement of high-strength steels. *Corrosion reviews*, 39(6), 487-517.

- [16] Anwar, S. (2020). Electrochemical and corrosion behavior of electrodeposited Zn, Zn-Ni alloy and Zn-Ni-TiO₂ (Doctoral dissertation, Memorial University of Newfoundland).
- [17] Maniam, K. K., & Paul, S. (2020). Progress in electrodeposition of zinc and zinc nickel alloys using ionic liquids. *Applied Sciences*, 10(15), 5321.
- [18] Costa, J. G. D. R. D., Costa, J. M., & Almeida Neto, A. F. D. (2022). Progress on electrodeposition of metals and alloys using ionic liquids as electrolytes. *Metals*, 12(12), 2095.
- [19] Maniam, K. K., Penot, C., & Paul, S. (2024). Influence of electrolyte choice on zinc electrodeposition. *Materials*, 17(4), 851.
- [20] Vignesh, R. V., & Sathiya, P. (2024). Sacrificial anode materials to protect marine grade steel structures: a review. *Corrosion Reviews*, 202(13), 2897-2904.
- [21] Saeedikhani, M., Wijesinghe, S. L., & Blackwood, D. J. (2019). Barrier and sacrificial protection mechanisms of zinc rich primers. *Engineering Journal*, 23(4), 223-233.
- [22] Dinakaran, R., Karthikeyan, S., Raja, K., & Jeeva, P. A. (2018). Improvement in corrosion resistance of mild steel using phosphate conversion coatings on electro-deposited alkaline zinc. *Materials Today: Proceedings*, 5(5), 13111-13118.
- [23] Nartita, R., Ionita, D., & Demetrescu, I. (2021). Sustainable coatings on metallic alloys as a nowadays challenge. *Sustainability*, 13(18), 10217.
- [24] Silva, R. M., Sperandio, G. H., da Silva, A. D., Okumura, L. L., da Silva, R. C., Moreira, R. P. L., & Silva, T. A. (2023). Electrochemically reduced graphene oxide films from Zn-C battery waste for the electrochemical determination of paracetamol and hydroquinone. *Microchimica Acta*, 190(7), 273.

- [25] Pereira, N. M., Pereira, C. M., Araujo, J. P., & Silva, A. F. (2017). Zinc electrodeposition from deep eutectic solvent containing organic additives. *Journal of Electroanalytical Chemistry*, 801, 545-551.